Cobalt-Catalyzed Carbon–Heteroatom Transfer Enables Regioselective Tricomponent 1,4-Carboamination

Kaitong Zhuang[a], Graham C. Haug[b], Yangyang Wang[a], Shuyu Yin[a], Huiying Sun[a], Siwen Huang[a], Ramon Trevino[b], Kunzhi Shen[c], Yao Sun[a], Chao Huang[a], Bin Qin[a], Yongxiang Liu[a], Maosheng Cheng[d], Oleg V. Larionov[b]*, and Shengfei Jin[a]*

[a] Wuya College of Innovation, Shenyang Pharmaceutical University, Shenyang 110016, P. R. China

[b] Department of Chemistry, University of Texas at San Antonio, San Antonio, Texas 78249, United States

[c] Shenyang Photosensitive Chemical Research Institute Co. Ltd., 8-12 No. 6 Road, Shenyang, 110141, P. R. China

[d] Key Laboratory of Structure-Based Drug Design and Discovery, Ministry of Education, School of Pharmaceutical Engineering, Shenyang Pharmaceutical University, Shenyang 110016, P. R. China

Email: jinshengfei@syphu.edu.cn, oleg.larionov@utsa.edu

ABSTRACT: Tricomponent cobalt(salen)-catalyzed carbofunctionalization of unsaturated substrates by radical-polar crossover has the potential to streamline access to broad classes of heteroatom-functionalized synthetic targets, yet the reaction platform has remained elusive, despite the well-developed analogous hydrofunctionalizations mediated by high-valent alkylcobalt intermediates. We report herein the development of a cobalt(salen) catalytic system that enables carbofunctionalization. The reaction entails a tricomponent decarboxylative 1,4-carboamination of dienes and provides a direct route to aromatic allylic amines by obviating preformed allylation reagents and protection of oxidation sensitive aromatic amines. The catalytic system merges acridine photocatalysis with cobalt(salen)-catalyzed regioselective 1,4-carbofunctionalization that facilitates the crossover of the radical and polar phases of the tricomponent coupling process, revealing critical roles of the reactants, as well as ligand effects and the nature of the formal high-valent alkylcobalt species on the chemo- and regioselectivity.

Introduction

Development of new catalytic systems has been one of the major driving forces that has transformed synthetic chemistry and dramatically increased accessibility of important synthetic intermediates, medicinal targets, and advanced materials.[1]

Metal-catalyzed hydrogen atom transfer (MHAT) reactions have enabled new approaches to functionalization of unsaturated substrates.[1c,2] In particular, cobalt(salen)-catalyzed reactions that combine MHAT with nucleophilic substitution in high-valent alkylcobalt(IV) intermediates have emerged as a versatile platform for chemo-, regio-, and stereoselective hydrofunctionalization of alkenes (Figure 1.A).[3-456] Mechanistically, the reaction is presumed to be initiated by the formation of putative cobalt(III) hydride that mediates MHAT to the alkene, producing alkylcobalt(III) via the intermediacy of the alkyl radical and cobalt(II) species. Subsequent oxidation to alkylcobalt(IV) enables the substitution reaction with a nucleophile.[2,3] The electrophilic character of the alkylcobalt(IV) intermediates is key to the alkyl group transfer to the nucleophile, although the reactivity and the nature of the high-valent species, and the effects of ligands remain poorly understood. Furthermore, given the central role of MHAT in the catalytic process, the scope of the reactions is confined to the net transfer of a hydrogen atom and a heteroatom-centered functional group to the unsaturated coupling partner.

Remarkably, the analogous tricomponent Co(salen)-catalyzed carbofunctionilization of unsaturated feedstocks has remained elusive (Figure 1.B).[7] Such a carbofunctionilization could enable a rapid buildup of molecular complexity and provide access to new chemical space by forging carbon–carbon and carbon–heteroatom bonds in a single, multicomponent transformation.

We hypothesized that the cobalt(salen)-catalyzed carbofunctionalization can be enabled by trapping of an appropriately generated alkyl radical by the cobalt(III) catalyst with subsequent addition to an unsaturated substrate, producing the alkylcobalt(IV) intermediate that transfers the alkyl group to the nucleophile.[8] However, the potential intermediacy of two alkylcobalt(IV) species pointed to the necessity of developing a catalytic system that could efficiently suppress the reaction with the nucleophile before the alkyl group transfer to the unsaturated substrate.

Given the central position of N-substituted aromatic amines in organic synthesis and drug discovery,[9] direct introduction of alkyl groups on the nitrogen atoms of unprotected aromatic amines has emerged at the forefront of synthetic methodology, and several methods have recently been developed[10] to address the limitations of the well-established reductive amination and alkylation reactions.[11] Allylic aromatic amines are important synthetic precursors that are typically accessed by a palladium-catalyzed allylation reactions, necessitating preformed allylic electrophiles.[12,13]

Conjugated dienes are synthetically versatile feedstocks that are readily accessible by a variety of synthetic methods[14] or produced industrially on multiton scales.[15] Carboamination of dienes is an emergent strategy that can enable simultaneous construction of C

–C and C–N bonds of a nitrogenous allylic system in a multicomponent fashion without prior assembly of an allylic fragment.[16-19] However, control of the regio- and stereoselectivity of diene carboamination has remained a challenge and has primarily been limited to 1,2-carboamination, while 1,4-carboamination has remained underdeveloped and has relied on palladium and other precious metals, with no examples of base metal catalytic systems. Notably, 1,4-carboaminaiton of dienes can be achieved under the Heck reaction conditions, entailing a sequence of two-electron processes.[16] However, the reaction scope is limited to

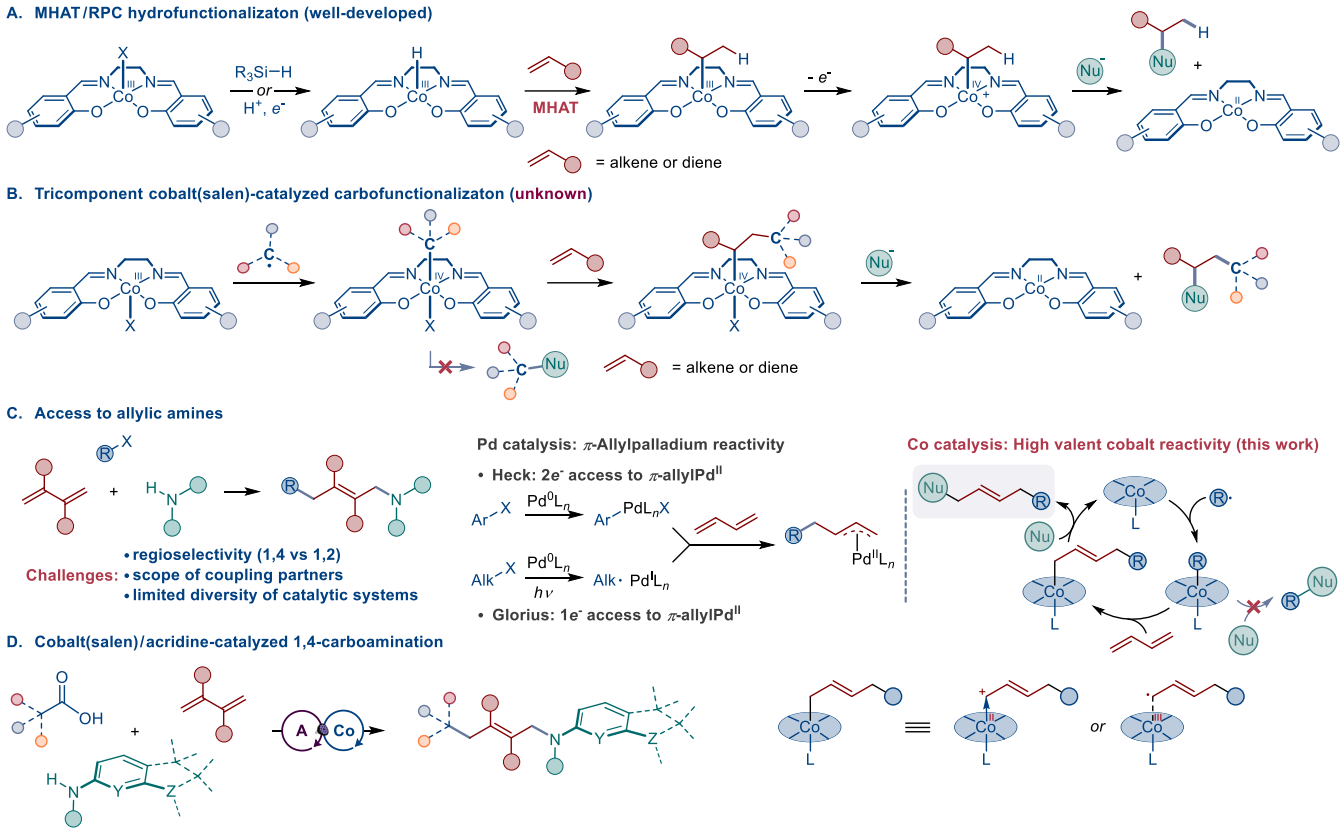

Figure 1. Cobalt(salen)-Catalyzed Tricomponent 1,4-Carboamination.

C(sp^2)–C bond formation from aryl and vinyl halides. Recently, a photocatalytic system based on photoinduced single electron transfer from Pd^0 has been developed by Glorius that has expanded the scope to C(sp^3)–C bond formation by facilitating alkyl radical generation from alkyl halides and redox-active esters.[17] Despite the progress, a base metal catalytic system that can enable a 1,4-regioselective installation of alkyl and amino groups on a diene moiety has remained elusive, limiting access to important allylic chemical space, e.g., allylic aromatic amines that cannot be directly accessed by the currently available multicomponent 1,4-carboamination methods.

We envisioned that a direct tricomponent decarboxylative coupling of carboxylic acids with dienes and unprotected anilines could provide a suitable catalytic system to develop the cobalt(salen)-catalyzed carbofunctionalization, because it can combine catalytic generation of alkyl radicals and allylcobalt(IV) intermediates that may facilitate the chemoselective carbon–heteroatom transfer to the unsaturated substrate in preference to the undesirable two-component alkylation of the nucleophile. Additionally, it would provide a one-step access to allylic aromatic amines (Figure 1.D), expanding their accessible chemical space as a consequence of the broad span of the chemical space of carboxylic acids across the domains of molecular complexity,[20] fraction of sp^3 carbon atoms (Fsp^3),[21] and geometric diversity.[22,23] The reaction would obviate the preactivation of carboxylic acids that is typically required to bypass the challenging and inefficient oxidation of carboxylic acids.[24-26] However, such a multicomponent reaction would require a merger of a photocatalytic system that can enable a direct generation of alkyl radicals from carboxylic acids with an allylation process that is kinetically and mechanistically fine-tuned to allow the formation of the allyl fragment from the diene prior to the reaction with aniline, diverting the system from the efficient and difficult-to-suppress alkyl radical- mediated N-alkylation (Figure 1.C).[10c] We report herein the direct decarboxylative tricomponent 1,4-carboamination of dienes that for the first time enables allylation of anilines with carboxylic acids and dienes by extending the Co(salen) catalysis to carbofunctionilization and without prior activation of carboxylic acids through a merger with acridine photocatalysis.[10c,22,25,26] The mechanistically distinct cobalt(salen) catalysis facilitates the tricomponent process, overcoming the competing N-alkylation, while an analysis of the formal high-valent Co^{IV}(salen) species points to the importance of the inverted ligand field effects and radical–metal interactions on the roles of ligands, as well as the nature, and reactivity of the cobalt-centered catalytic species.

Table 1. Tricomponent decarboxylative 1,4-carboamination [a]

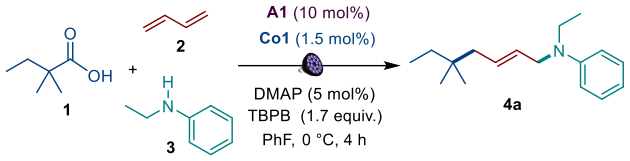

Entry	Variations from standard conditions	Yield, % [b]
1	none	90 (91)[c]
2	With **Co2**	86
3	no light, **A1**, **Co1**, or TBPB	–
4	At 25 °C	23
5	MeCN instead of PhF	trace
6	**A2** or **A3** instead of **A1**	45
7	With **Co3**	58
8	With **Co4**	82
9	With **Co5**	76
10	No DMAP	70
11	Ph_3P instead of DMAP	77

[a] Reaction conditions: acid **1** (0.3 mmol), diene **2** (0.3 mmol), aniline **3** (0.2 mmol), **A1** (10 mol%), **Co1** (1.5 mol%), DMAP (5 mol%), TBPB (0.34 mmol), PhF (3 mL), LED light (400 nm, 2.6 mW/cm^2), 4 h. [b] Yields were determined by ^{1}H NMR with 1,4-dimethoxybenzene as an internal standard. [c] Isolated yield. TBPB = *tert*-butyl peroxybenzoate. DMAP = 4-Dimethylaminopyridine.

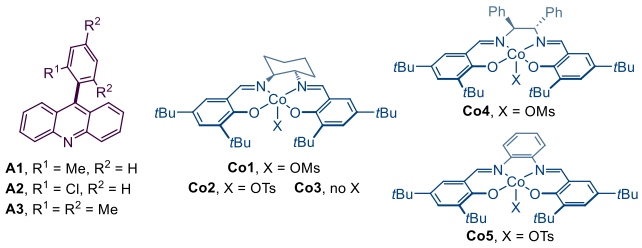

Results and Discussion

Optimization studies revealed that a reaction of carboxylic acid **1**, diene **2**, and aniline **3** afforded 1,4-carboamination product **4a** in 90% and with complete stereoselectivity and regioselectivity in fluorobenzene as a solvent and in the presence of acridine **A1** and Co^{III} salen complex **Co1** as catalysts (Table 1, entry 1). The reaction was conducted with DMAP as a ligand to stabilize the high-valent cobalt catalytic species.[27] Other cobalt(salen) sulfonate complexes demonstrated similar catalytic activity (entry 2). Control experiments in the absence of light, acridine, cobalt, and the oxidant indicated that these reaction parameters were crucial to the formation of 1,4-carboamination product **4a** (entry 3). Higher reaction temperatures led to a decreased yield, likely due to diene polymerization (entry 4). Similarly, other solvents (entry 5), as well as other acridine and cobalt catalysts, and ligands (entries 6–10) provided lower yields, resulting in increased undesirable decomposition of the coupling partners and polymerization.

With the optimized conditions in hand, we next studied the applicability of the direct decarboxylative 1,4-carboamination of

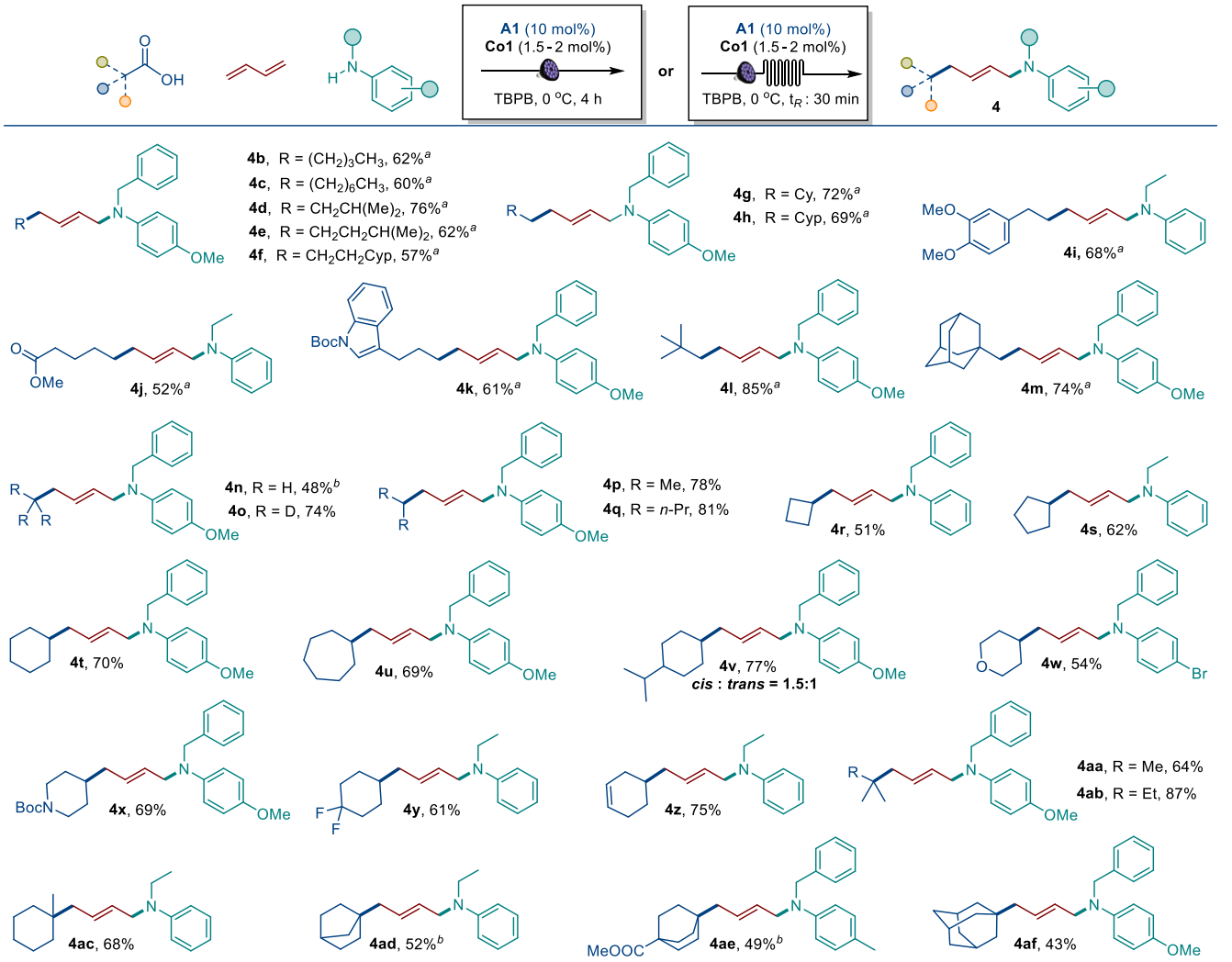

Scheme 1. Scope of carboxylic acids in the acridine/cobalt catalyzed 1,4-carboamination of 1,3-dienes. Reaction conditions: acid **1** (0.3–0.4 mmol), diene **2** (0.3 mmol), aniline **3** (0.2 mmol), **A1** (10–20 mol%), **Co1** or **Co2** (1.5–2 mol%), DMAP (5 mol%), TBPB (0.34 mmol), PhF (3 mL), LED light (400 nm, 2.6 mW/cm^2), 4 h, isolated yields. [a] Benzene/MeCN (3 : 1, 3 mL) was used as solvent. [b] Reaction was carried out in flow.

1,3-dienes. First, the scope of carboxylic acids was explored (Scheme 1). Primary, secondary, and tertiary acids were all compatible, and the products were obtained in 4 hours with excellent yields and complete stereo- and regiocontrol. Primary aliphatic carboxylic acids (**4b-4h, 4l-4m**) as well as acids bearing aryl, ester, carbamate, and heterocyclic functionalities were directly converted to the products in good yields (**4i–4k**). Acetic acid (**4n**) and deuterated acetic acid (**4o**) were also well-tolerated, with the latter product demonstrating a straightforward installation of a trideuteriomethyl group in a tricomponent reaction that can be useful for applications in medicinal chemistry.[28] Various acyclic and cyclic secondary carboxylic acids were also tested (**4p-4v**) including a strained small ring (**4r**). Heterocyclic fragments such as tetrahydropyran (**4w**) and Boc-protected piperidine (**4x**) were compatible with the decarboxylative tricomponent reaction. In addition, fluorinated (**4y**) and unsaturated (**4z**) substrates could also be used in the reaction. Furthermore, a range of tertiary acids readily produced *trans*-alkenes bearing both cyclic and acyclic tertiary alkyl groups in good yields (**4aa-4af**). The reaction could also be conducted as a continuous-flow process. Allylic amines **4n**, **4ad**, and **4ae** were readily prepared under continuous flow conditions with a residence time of 30 min.

The scope of the transformation with respect to the aniline substrate was also examined (Scheme 2). A variety of primary anilines were tested first (**5a-5h**). Experiments revealed that the reaction tolerates sterically encumbered (**5a** and **5b**) and diversely substituted anilines (**5d-5h**). N-Alkylated anilines bearing thioether, halogen, and ester groups as well as heterocyclic frameworks were also suitable coupling partners (**5m-5v**). Additionally, several diarylamines were successfully converted to the corresponding allylic amines (**5w-5y**). Notably, the reaction could be carried out on a 6 mmol scale under continuous-flow conditions, providing gram quantities of allylic amine **5i**. The flow synthesis

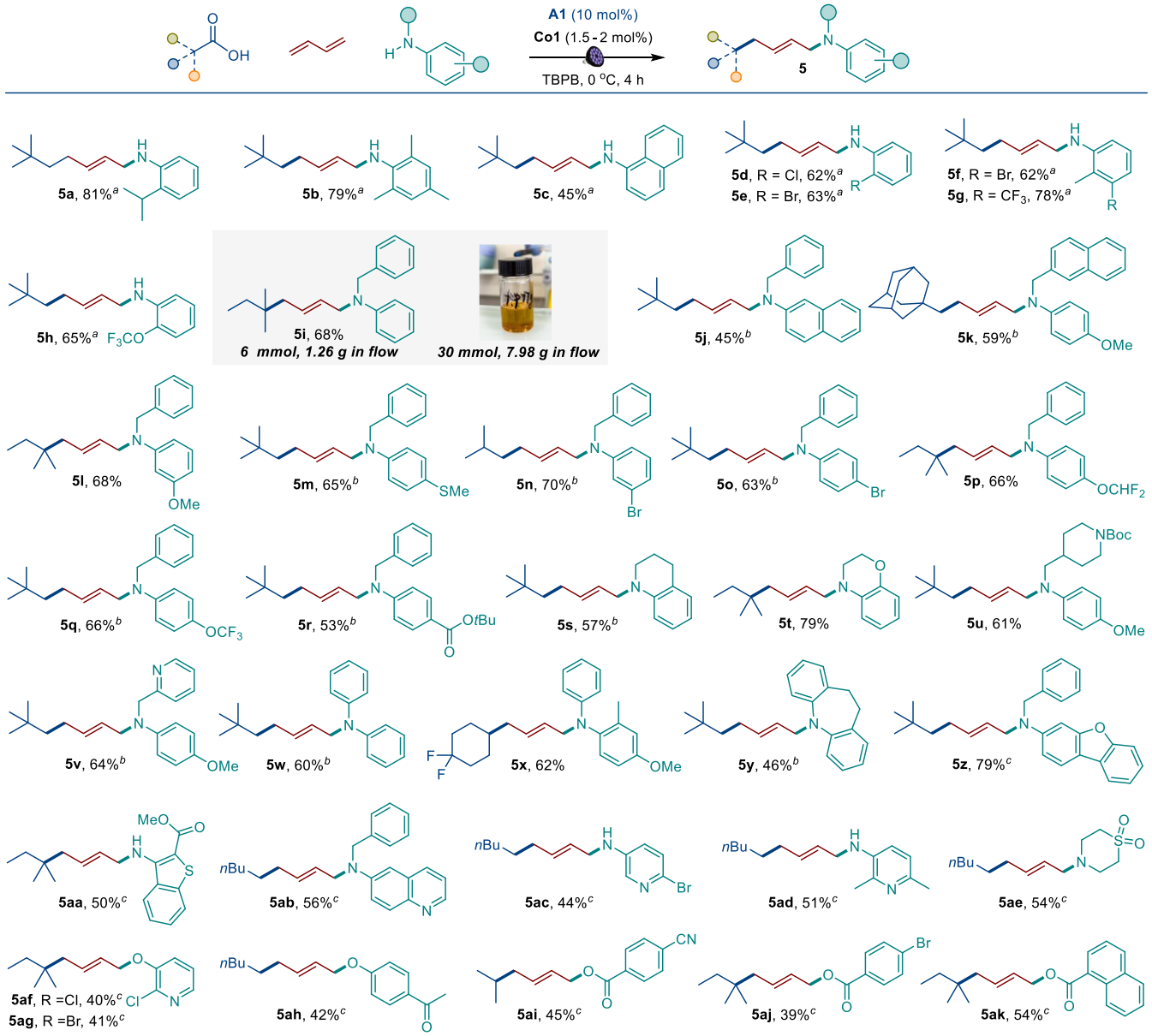

Scheme 2. Scope of amines in the acridine/cobalt catalyzed 1,4-carboamination of 1,3-dienes. Reaction conditions: see Scheme 1, isolated yields. [a] Aniline / acid = 3 : 1. [b] benzene/MeCN (3 : 1, 3 mL). [c] See supporting information for specific reaction conditions.

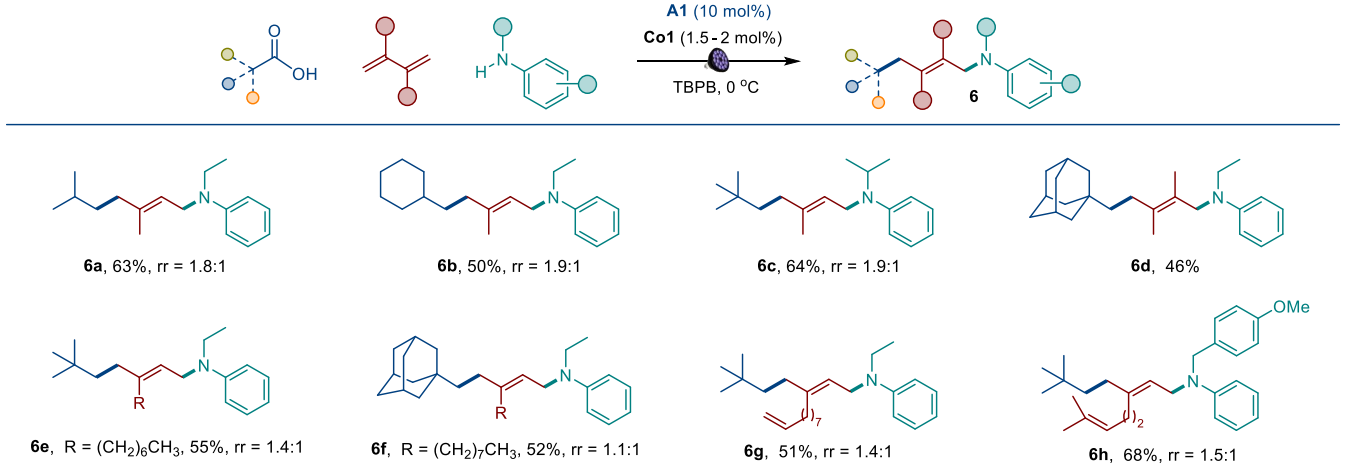

Scheme 3. Scope of dienes in the acridine/cobalt-catalyzed 1,4-carboamination of 1,3-dienes. Reaction conditions: acid **1** (0.3–0.4 mmol), diene **2** (0.3 mmol), aniline **3** (0.2 mmol), **A1** (10–20 mol%), **Co1** or **Co2** (1.5–2 mol%), DMAP (5 mol%), TBPB (0.34 mmol), benzene/MeCN (3 : 1, 3 mL), LED light (400 nm, 2.6 mW/cm²), 4 h, isolated yields.

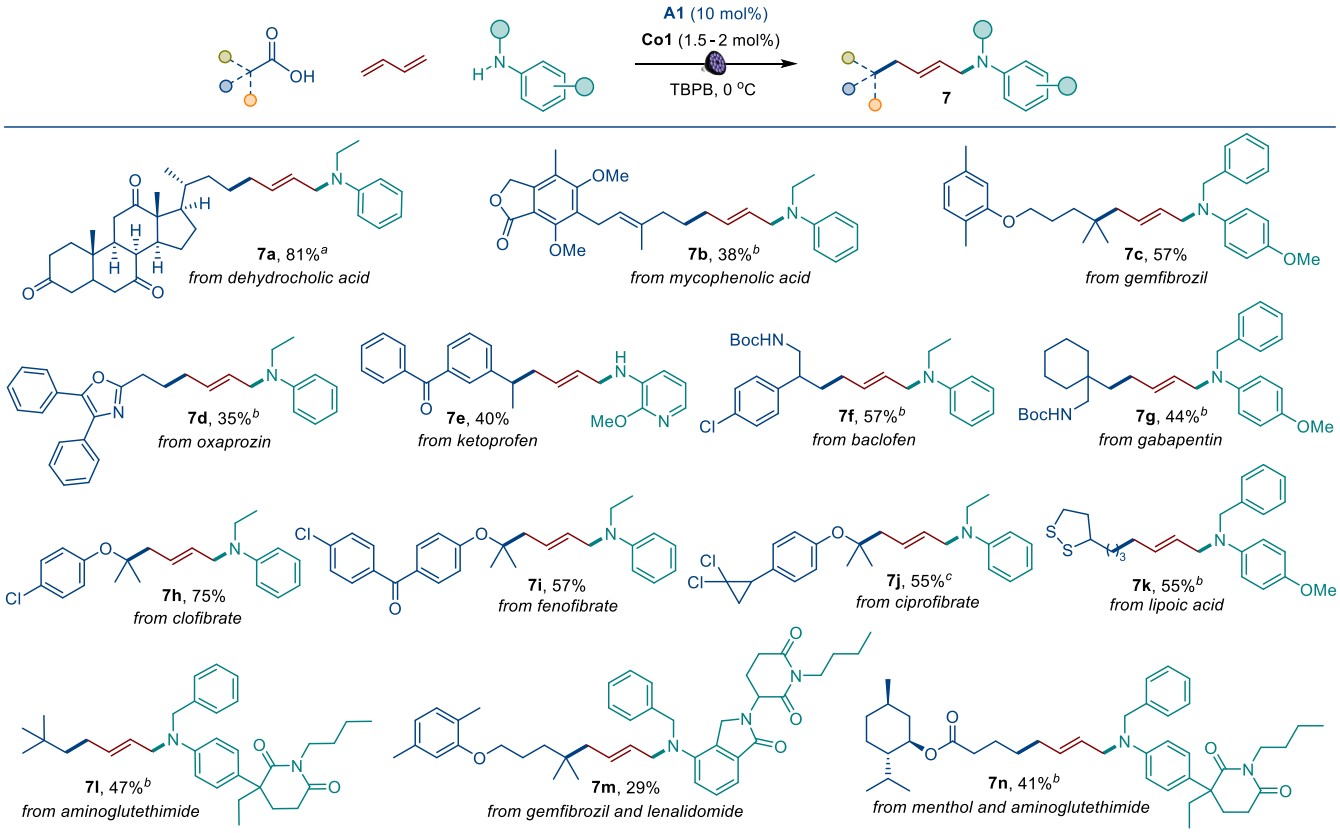

Scheme 4. Structural modification of natural products and medicinal products. Reaction conditions: acid **1** (0.3–0.4 mmol), diene **2** (0.3 mmol), aniline (0.2 mmol), **A1** (10–20 mol%), **Co1** or **Co2** (1.5–2 mol%), DMAP (5 mol%), TBPB (0.34 mmol), PhF (3 mL), LED light (400 nm, 2.6 mW/cm^2), 4 h, isolated yields. [a] PhF/DCM (1 : 1, 3 mL), [b] Benzene/MeCN (3 : 1, 3 mL). [c] Reaction was carried out in flow.

of **5i** can be further scaled up to 30 mmol (86% isolated yield, 1 g · h^{-1} production rate), enabling production at a higher concentration (0.15 M). In addition to carbocyclic aromatic amines, an array of heteroaromatic amines including dibenzofuran (**5z**), benzothiophene (**5aa**), quinoline (**5ab**), and substituted pyridines (**5ac** and **5ad**) were tolerated. A product derived from a cyclic aliphatic amine was also readily obtained (**5ae**). Furthermore, oxygen-centered nucleophiles, such as (hetero)aromatic phenols (**5af-5ah**) and aromatic carboxylic acids (**5ai-5ak**) were efficiently introduced, with **Co4** and **Co5** as optimal cobalt catalysts, indicating that the catalytic system can be further fine-tuned to accommodate other nucleophiles.

The scope of dienes was evaluated next (Scheme 3). Under the optimal conditions, simple feedstock dienes, such as isoprene (**6a-6c**), 2,3-dimethyl-1,3-butadiene (**6d**), and myrcene (**6h**) were all converted to the desired products. Several 1,3-dienes bearing saturated and unsaturated aliphatic substituents were also evaluated (**6e-6g**), and the corresponding allylic amine motifs were obtained in moderate yields. For 2-substituted dienes, the major regioisomer featured the amino group at the less substituted diene double bond, in line with the kinetically favored addition of the alkyl radical to the more substituted diene double bond that leads to the formation of the more stable allyl radical intermediate (Scheme S1 in SI).

To further showcase the functional group tolerance and utility of the developed transformation, several natural products and active pharmaceutical ingredients were also converted to their corresponding 1,4-carboamination products (Scheme 4). Dehydrocholic acid and mycophenolic acid (**7a**, **7b**) readily produced corresponding products, pointing to a good compatibility with ketones and lactones. Pleasingly, antihyperlipidaemic gemfibrozil (**7c**), anti-inflammatory oxaprozin (**7d**) and ketoprofen (**7e**), anticonvulsant gabapentin (**7f**), and antispasmodic baclofen (**7g**) were all suitable substrates, demonstrating good functional group tolerance. Moreover, several antilipidemic agents, e.g., clofibrate (**7h**), fenofibrate (**7i**), and ciprofibrate (**7j**) afforded the 1,4-carboamination products without any detriment to the pendant functional groups under batch and flow conditions. Remarkably, lipoic acid was also smoothly converted to allylic amine **7k** leaving the radical- and oxidation-sensitive disulfide bridge unaffected. Furthermore, medicinally important amines, e.g., a derivative of the aromatase inhibitor aminoglutethimide (**7l**) was readily alkylated in good yield. Interestingly, gemfibrozil and lenalidomide could be linked together by a rigid tether using the developed method (**7m**), pointing to potential medicinal applications in the context of construction of proteolysis targeting chimera (PROTAC).[29] Similarly, menthol and aminoglutethimide were combined in good yield (**7n**), indicating that diverse linchpins can be designed based on the carboamination strategy.

We next conducted experimental and computational studies to clarify the sequence of processes that underlie the dual catalytic 1,4-carboamination (Figure 2). Addition of TEMPO resulted in suppression of 1,4-carboamination, and the corresponding product of the alkyl radical trapping by TEMPO (**T1**) was produced in 76% yield (Figure 2.A), indicating that the reaction proceeds through

decarboxylative alkyl radical generation, with further experiments pointing to acridine photocatalysis as the underlying process for the carboxylic acid conversion to the alkyl radical intermediate (Tables S4–S7 and the discussion in the SI). Notably, no product of trapping of the allyl radical with TEMPO **T2** was observed with 3 equiv. and substoichiometric (20 mol%) loadings of TEMPO, suggesting that the alkyl radical is trapped by the cobalt complex that is then converted to the reactive allylcobalt intermediate through a reversible Co–C homolysis and rapid (e.g., in cage)[30] uptake of the diene. Indeed, the corresponding alkylcobalt(salen) species was detected mass spectroscopically, indicating that the alkyl radical is intercepted by the cobalt catalyst (Figure 2.B). These results are congruent with the previously established persistent radical reactivity observed for cobalt complexes.[25a,31] The role of aniline was investigated next. A Job plot study for the aniline–cobalt catalyst system indicated that aniline does not form a complex with the cobalt catalyst under the reaction conditions (Table S1). On the other hand, a negative slope of the Hammett plot for substituted anilines suggested that aniline has a nucleophilic role in the catalytic process (Figure 2.C). To this end, a reaction of alkylcobalt(III) complex **Co6** with aniline **8** in the presence of TBPB produced corresponding N-alkylated aniline **9** in similar yields in the dark and under LED irradiation. Given the lower oxidation potential of complex **Co6** (E_{ox} = 0.55 V vs SCE in DCM for Co complex **Co6** and 0.85 V for aniline **8**, Figures S1 and S2), these results point to the

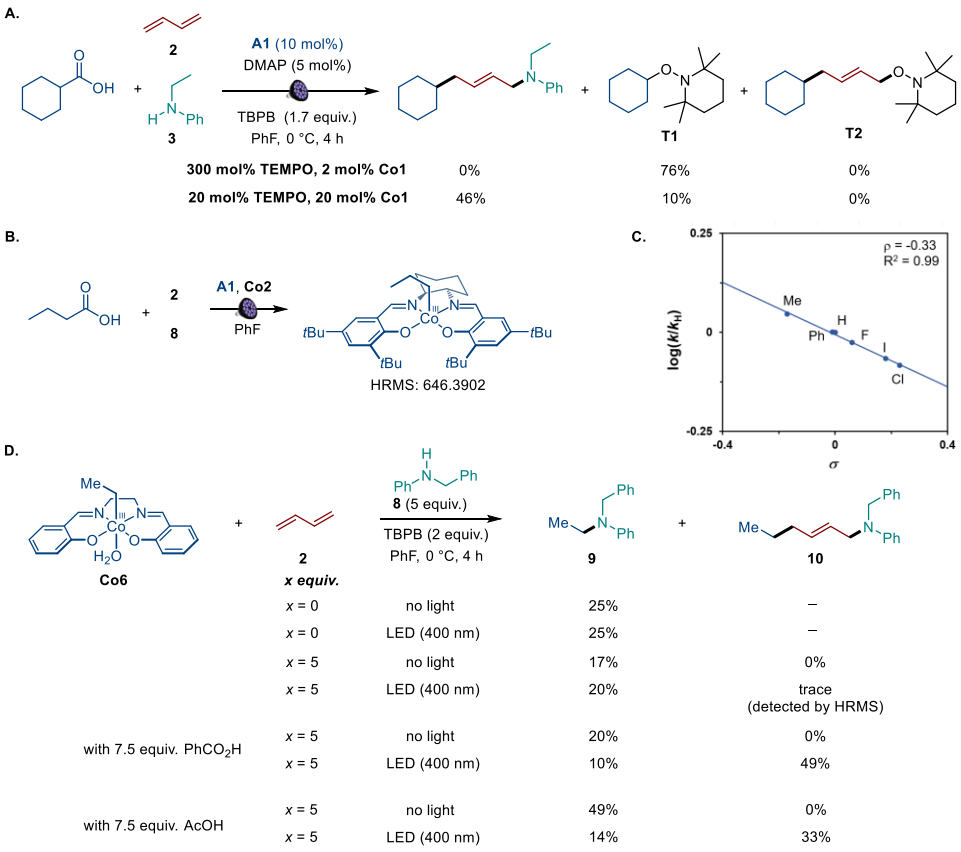

Figure 2. Mechanistic studies of the dual catalytic 1,4-carboaminaiton. **A.** Radical trapping studies with TEMPO. **B.** Mass-spectroscopic detection of the alkylcobalt intermediate. **C.** Hammett plot for the substituent effects in the aniline reactant. **D.** Reactions of alkylcobalt(III) **Co6** with aniline **8**.

involvement of formal alkylcobalt(IV) species in a thermally induced oxidative coupling with anilines. Interestingly, addition of butadiene to the reaction of cobalt complex **Co6** and aniline **8** did not produce 1,4-carboamination product **10** in the absence of light, while only traces of product **10** were detected by mass spectroscopy under LED irradiation. Instead, direct N-alkylation product **9** was formed. Significantly, when the reaction was carried out in the presence of a carboxylic acid and under LED irradiation, allylamine **10** became the major product.[32] This result suggests that the acid acts as an inhibitor of the undesirable direct N-alkylation pathway by forming a hydrogen bond-complex with the aniline, thus reducing the concentration of the aniline that is available for the N-alkylation and permitting the light-induced reaction of diene with cobalt complex **Co6** to be kinetically competitive. Given the facility of the observed oxidative conversion of **Co6** in the presence of TBPB, these results suggest that the formation of the allylcobalt intermediate takes place after the oxidation of the alkylcobalt species by a photoinduced homolysis of the weak Co–C bond (e.g., BDE 23.5 kcal/mol[33]), as previously observed for alkylcobalt complexes.[25,31b] Supporting this conclusion, TD-DFT calculations indicate that alkylcobalt(IV) species absorb light in the emission range of the LED source (Figure S3). Importantly, no reaction was observed in any of the experiments in the absence of TBPB, ruling out a N-allylation mechanism wherein alkylcobalt(III) adds to the diene via a reversible Co–C homolysis and alkyl radical addition with subsequent nucleophilic attack of aniline on the intermediate allylcobalt(III) that leads to N-allylation and generation of Co(I). (Figure S10). To gain insight into the mechanism of the reaction and the nature of the processes that involve formal high-valent Co^{IV} species, computational studies were carried out next (Figure 3). As suggested by the experimental observations, after the homolytic dissociation of an alkylcobalt(IV) in-

termediate (vide supra), addition of the alkyl radical to diene **2** proceeded exergonically over a readily accessible barrier (**TSA**), producing allyl radical **11**. The ensuing coupling of radical **11** with catalytic Co^{III}(salen) mesylate complex **12** demonstrated high selectivity (cf., **TSB** and **TSC**) for the linear addition product, i.e., formal Co^{IV} allylcobalt intermediate **13**, in line with the experimental observations, with the branched product **14** also being substantially less stable.

The Co–C distance in the more energetically favorable linear **TSB** is significantly shorter than in the branched **TSC** (cf., 2.23 Å and 3.11 Å). Activation strain model (ASM) distortion/interaction analysis[34] of **TSB** and **TSC** indicates that transition state **TSB** has a significantly higher distortion energy reflective of the shorter distance between the cobalt fragment and the less substituted terminus of the allyl group in **TSB**, and with a greater contribution from the distortion of the cobalt fragment in both transition states. The greater distortion in **TSB** is, however, compensated by a substantially higher interaction energy. The Energy Decomposition Analysis[35] (EDA) suggests that the shorter interfragment distance in **TSB** results in a stronger Pauli (steric) repulsion that is counterbalanced by even stronger attractive interactions, especially charge transfer (i.e., orbital interactions between the fragments) and electrostatic interactions (i.e., Coulombic interactions between the charge distributions of the fragments), that also benefit from the proximity of the reacting fragments in **TSB**. By contrast, dispersion has a comparatively smaller contribution to the stabilizing interactions.

The out-of-sphere substitution reaction of allylcobalt intermediates **13** and **14** with aniline was kinetically facile (**TSD** and **TSE**), affording *N*-allylanilinium intermediates **16** and **17** that proceeded to produce aniline products **18** and **19** after exergonic deprotonation with the oxidant-derived benzoate. The Co^{II} complex **20** that was produced in the reaction of Co^{IV} intermediate **13** with aniline underwent a low-barrier ($\Delta G^{\neq}_{SET}$ = 7.4 kcal/mol) oxidation by TBPB to the catalytic Co^{III} complex **12** via a concerted single electron transfer. The generated *tert*-butoxy radical facilitates the turnover of the acridine photocatalyst by a hydrogen atom transfer from the acridinyl radical produced in the photocatalytic decarboxylation.[22a]

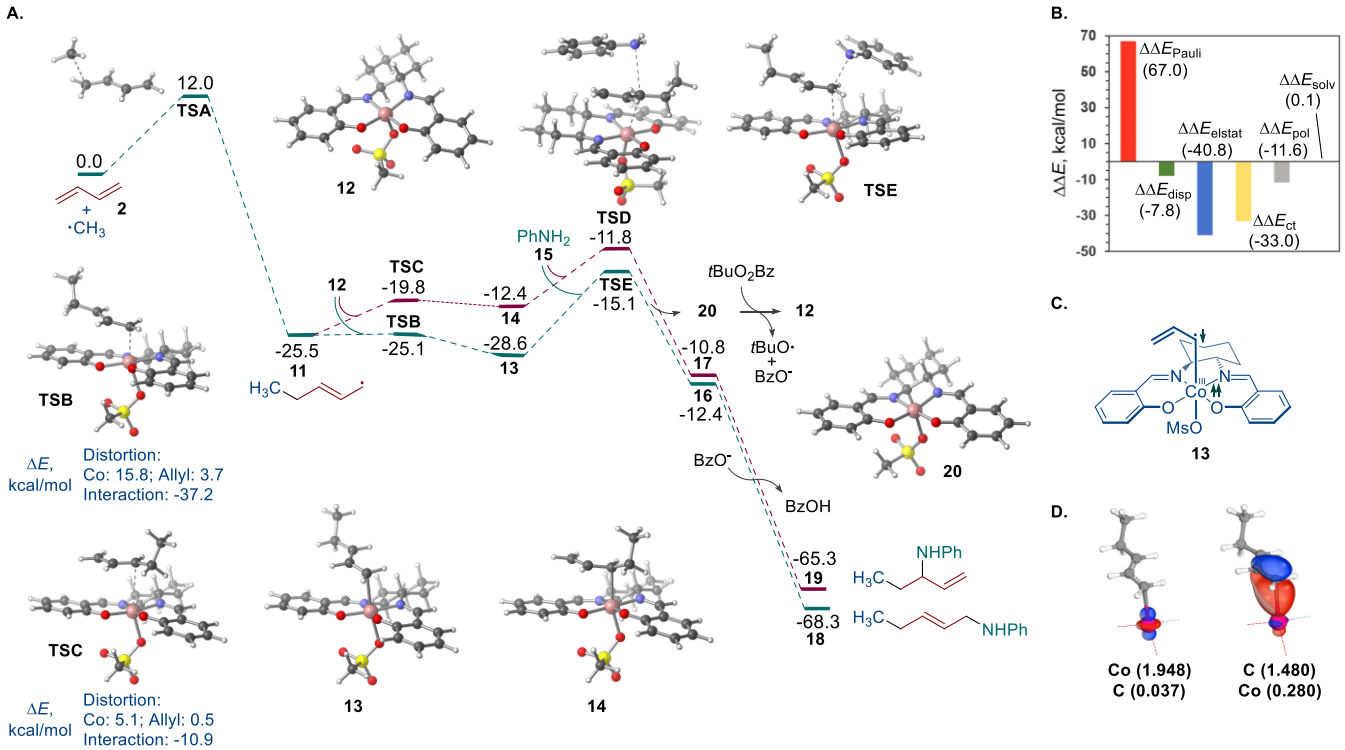

Figure 3. Computational studies of the 1,4-carboaminaiton. **A.** Gibbs free energy profile of the 1,4-carboaminaiton, kcal/mol, PW6B95-D3(BJ)/def2-SVP(H,C,O,N,S,Cl)/def2-TZVP(Co)/SMD(PhF)//PW6B95-D3(BJ)/def2-TZVP/SMD(PhF). **B.** Energy decomposition analysis for the allyl radical addition, $\Delta\Delta E^{\neq} = \Delta E^{\neq}_{TSB} - \Delta E^{\neq}_{TSC}$, kcal/mol. **C.** Spin distribution in mesylate **13**. **D.** IBOs describing the Co–C bond in mesylate **13**.

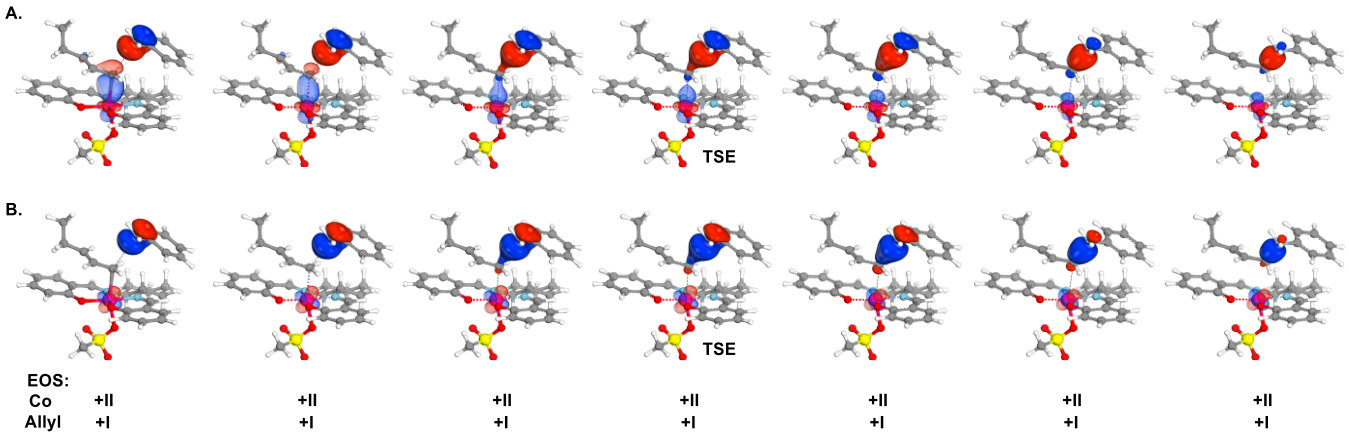

Figure 4. Transformation of the Co–C (transparent) and C–N (solid) IBOs in the α (**A**) and β (**B**) space along the IRC for the reaction of intermediate **13** with aniline.

To further clarify the oxidation state and reactivity of the Co^{IV} species involved in the reaction, effective oxidation state (EOS)[36] and intrinsic bond orbital (IBO)[37] analyses of intermediate **13** and the aniline substitution transition state **TSE** were carried out. The EOS analysis suggested that the oxidation state in the formal Co^{IV} intermediate **13** can be described as a triplet Co^{III} center antiferromagnetically coupled to an allyl radical (Figure 3.C). This assignment is supported by the partial spin of 1.67 on the Co center and –0.79 on the allyl group. Concurringly, the IBO analysis indicates that, in addition to the one singly and two doubly occupied d-orbitals, the IBOs corresponding to the Co–C bond are mainly cobalt-centered in the α space and carbon-centered in the β space (Figure 3.D), in contrast to the IBOs of the Co–O and Co–N bonds that are clearly dative, as revealed by the partial charges, predominantly residing on the heteroatoms (Figure S15). Interestingly, the oxidation state of the cobalt center changes to Co(II) with the spin mainly residing on the Co center and the allyl group featuring an overall oxidation state of +I early en route to transition state **TSE** in the reaction with aniline (Figure 4). The IBO analysis indicates that the α-IBO associated with the Co–C bond is transformed into the cobalt d-orbital along the IRC, while the IBOs corresponding to the nitrogen lone pair become the C–N bond, pointing to a process that can be described as single-electron transfer from the allyl group to the cobalt center. Given the possibility of the mesylate dissociation from complex **13** or a displacement of the mesylate with an L-type ligand (e.g., DMAP), the reactivities and oxidation states of the pentacoordinate cationic species **21** and hexacoordinate pyridine complex **22** were also

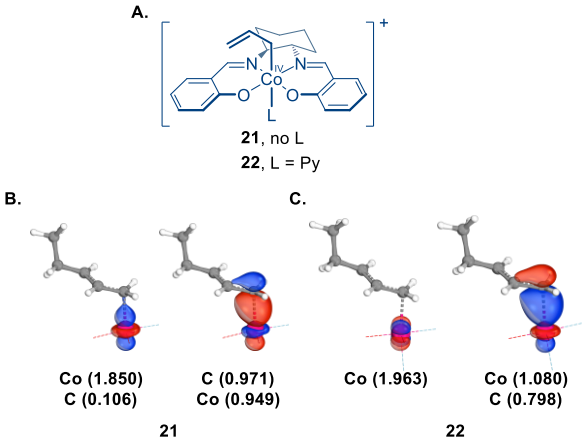

Figure 5. A. Co^{IV}(salen) complexes **21** and **22**. **B.** IBOs describing the Co–C bond in complex **21**. **C.** IBOs describing the Co–C bond in complex **22**.

studied (Figure 5). Recent studies on the nature of carbon–metal bonding in formally high oxidation state metal complexes of copper, nickel, and cobalt pointed to the importance of the inverted ligand field, wherein the carbon–metal bonding orbitals are dominated by the metal, giving the bond an inverted polarity that can be described as a metal electron pair donation to a carbocation, in contrast to the classical Werner-type ligand-to-metal coordination.[3k,38] The EOS analysis indicated that the metal center in the formal Co^{IV} complex **21** is best described as Co^{II} with the allyl group featuring an oxidation state of +I, in line with the earlier studies.[3k] The conclusion is supported by the IBO analysis that reveals a partial spin of 1.29 on Co and –0.38 on the allyl group. Furthermore, the dominant contribution of cobalt to the Co–C bond IBOs as indicated by the partial charges also points to the presence of an inverted ligand field (Figure 5.B), while cationic pyridine complex **22** occupies an intermediate position between mesylate **13** and complex **21** (Figure 5.C). Notably, transition states leading to linear product **18** from intermediates **21** and **22** remain energetically preferred regardless of the coordination mode (Figure S26), indicating that the experimentally observed selectivity can be attained with any of the formal Co^{IV} intermediates. These results underscore the influence of the ligand effects on the oxidation state of the cobalt in formal cobalt(IV) complexes and the common features of their reactivities in out-of-sphere nucleophilic substitutions.

Taken together, the experimental and computational studies indicate that the acridine and cobalt catalytic cycles can be interfaced through an alkyl radical interception by Co^{III}(salen) **C** producing formal cobalt(IV) intermediate **D** (Figure 6). The weak Co–C bond in intermediate **D** can readily undergo photoinduced homolysis leading to reversible regeneration of the alkyl radical with subsequent production of allyl radical **E** upon addition to the diene and formation of allylcobalt(IV) intermediate **F**. The ensuing nucleophilic substitution affords Co^{II} complex **G**. The catalyst turnover via a single electron transfer to the oxidant furnishes the *tert*-butoxy radical that regenerates the acridine catalyst from the acridinyl radical **HA**, facilitating the subsequent alkyl radical production from the carboxylic acid by photoinduced proton-coupled electron transfer in hydrogen bond complex **B**, as descried in previous mechanistic studies of acridine photocatalysis.[25] In addition, Co^{II} complex **G** can also couple with the alkyl radical, producing alkylcobalt(III) intermediate **H** that undergoes oxidation to intermediate **D**, in line with the experimental observations.

Conclusion

In conclusion, we have developed a hitherto unexplored cobalt(salen)-catalyzed carbofunctionalization that enables a direct decarboxylative tricomponent 1,4-carboamination of dienes providing access to aromatic allylic amines from carboxylic acids without the need for carboxylic acid preactivation, use of preformed allylic fragments, or protection of oxidation sensitive amine precursors. The reaction is facilitated by a successful merger of acridine photocatalysis with cobalt(salen)-catalyzed carbofunctionalization. The mild reaction conditions allow for engaging a broad range of carboxylic acids, aromatic amines, and dienes under batch and flow conditions. Furthermore, our studies point to key roles of the radical and polar reactivity of the cobalt catalyst in determining the chemo- and regioselective outcomes of the process, as well as the reactivity-modulating role of carboxylic acids, and clarify the nature of the oxidation states of the cobalt-centered catalytic species.

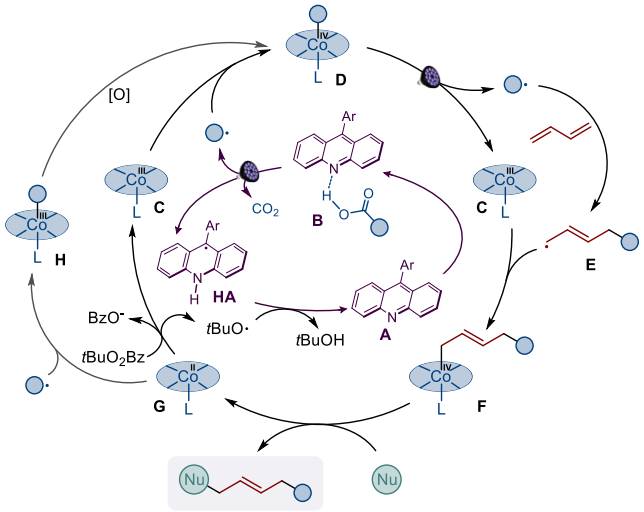

Figure 6. Mechanism of the direct decarboxylative 1,4-carboamination.

Notes

The authors declare no competing financial interest.

ACKNOWLEDGMENT

S.J. thanks the National Natural Science Foundation of China (No. 22101187). O.V.L. acknowledges the Welch Foundation (AX-0047), the Texas Advanced Computing Center (TACC), and Advanced Cyberinfrastructure Coordination Ecosystem: Services & Support (ACCESS).

REFERENCES

(1) (a) Yudin, A. K., Ed. *Catalyzed Carbon-Heteroatom Bond-Formation;* Wiley-VCH: Weinheim, **2010**. (b) Hönig, M.; Sondermann, P.; Turner, N. J.; Carreira, E. M. Enantioselective Chemo- and Biocatalysis: Partners in Retrosynthesis. *Angew. Chem., Int. Ed.* **2017**, *56*, 8942–8973. (c) Green, S. A.; Crossley, S. W. M.; Matos, J. L. M.; Vásquez-Céspedes, S.; Shevick, S. L.; Shenvi, R. A. The High Chemofidelity of Metal-Catalyzed Hydrogen Atom Transfer. *Acc. Chem. Res.* **2018**, *51*, 2628–2640. (d) Lam, N. Y. S.; Wu, K.; Yu, J. Q. Advancing the Logic of Chemical Synthesis: C–H Activation as Strategic and Tactical Disconnections for C–C Bond Construction. *Angew. Chem., Int. Ed.* **2021**, *60*, 15767–15790.

(2) Crossley, S. W. M.; Obradors, C.; Martinez, R. M.; Shenvi, R. A. Mn-, Fe-, and Co-Catalyzed Radical Hydrofunctionalizations of Olefins. *Chem. Rev.* **2016**, *116*, 8912–9000.

(3) (a) Shigehisa, H.; Aoki, T.; Yamaguchi, S.; Shimizu, N.; Hiroya, K. Hydroalkoxylation of Unactivated Olefins with Carbon Radicals and Carbocation Species as Key Intermediates. *J. Am. Chem. Soc.* **2013**, *135*, 10306–10309. (b) Shigehisa, H.; Koseki, N.; Shimizu, N.; Fujisawa, M.; Niitsu, M.; Hiroya, K. Catalytic Hydroamination of Unactivated Olefins Using a Co Catalyst for Complex Molecule Synthesis. *J. Am. Chem. Soc.* **2014**, *136*, 13534–13537. (c) Shigehisa, H.; Hayashi, M.; Ohkawa, H.; Suzuki, T.; Okayasu, H.; Mukai, M.; Yamazaki, A.; Kawai, R.; Kikuchi, H.; Satoh, Y.; Fukuyama, A.; Hiroya, K. Catalytic Synthesis of Saturated Oxygen Heterocycles by Hydrofunctionalization of Unactivated Olefins: Unprotected and Protected Strategies. *J. Am. Chem. Soc.* **2016**, *138*, 10597–10604. (d) Touney, E. E.; Foy, N. J.; Pronin, S. V. Catalytic Radical Polar Crossover Reactions of Allylic Alcohols. *J. Am. Chem. Soc.* **2018**, *140*, 16982–16987. (e) Zhou, X. L.; Yang, F.; Sun, H. L.; Yin, Y. N.; Ye, W. T.; Zhu, R. Cobalt-Catalyzed Intermolecular Hydrofunctionalization of Alkenes: Evidence for a Bimetallic Pathway. *J. Am. Chem. Soc.* **2019**, *141*, 7250–7255. (f) Vrubliauskas, D.; Vanderwal, C. D. Cobalt-Catalyzed Hydrogen-Atom Transfer Induces Bicyclizations that Tolerate Electron-Rich and Electron-Deficient Intermediate Alkenes. *Angew. Chem., Int. Ed.* **2020**, *59*, 6115–6121. (g) Ebisawa, K.; Izumi, K.; Ooka, Y.; Kato, H.; Kanazawa, S.; Komatsu, S.; Nishi, E.; Shigehisa, H. Catalyst- and Silane-Controlled Enantioselective Hydrofunctionalization of Alkenes by Cobalt-Catalyzed Hydrogen Atom Transfer and Radical-Polar Crossover. *J. Am. Chem. Soc.* **2020**, *142*, 13481–13490. (h) Yin, Y.-N.; Ding, R.-Q.; Ouyang, D.-C.; Zhang, Q.; Zhu, R. Highly chemoselective synthesis of hindered amides via cobalt-catalyzed intermolecular oxidative hydroamidation. *Nat. Commun.* **2021**, *12*, 2552. (i) Qin, T.; Lv, G.; Meng, Q.; Zhang, G.; Xiong, T.; Zhang, Q. Cobalt-Catalyzed Radical Hydroamination of Alkenes with *N*-Fluorobenzenesulfonimides. *Angew. Chem., Int. Ed.* **2021**, *60*, 25949–25957. (j) Fischer, D. M.; Balkenhohl, M.; Carreira, E. M. Cobalt-Catalyzed Cyclization of Unsaturated *N*-Acyl Sulfonamides: a Diverted Mukaiyama Hydration Reaction. *JACS Au* **2022**, *2*, 1071–1077. (k) Wilson, C. V.; Kim, D.; Sharma, A.; Hooper, R. X.; Poli, R.; Hoffman, B. M.; Holland, P. L. Cobalt–Carbon Bonding in a Salen-Supported Cobalt(IV) Alkyl Complex Postulated in Oxidative MHAT Catalysis. *J. Am. Chem. Soc.* **2022**, *144*, 10361–10367. (l) Ye, W.-T.; Zhu, R. Dioxygen-promoted cobalt-catalyzed oxidative hydroamination using unactivated alkenes and free amines. *Chem. Catal.* **2022**, *2*, 345–357. (m) Hoogesteger, R. H.; Murdoch, N.; Cordes, D. B.; Johnston, C. P. Cobalt-catalyzed Wagner–Meerwein rearrangements with concomitant nucleophilic hydrofluorination. *Angew. Chem. Int. Ed.* **2023**, e202308048. (n) Park, S. H.; Bae, G.; Choi, A.; Shin, S.; Shin, K.; Choi, C. H.; Kim, H. Electrocatalytic Access to Azetidines Via Intramolecular Allylic Hydroamination: Scrutinizing Key Oxidation Steps through Electrochemical Kinetic Analysis. *J. Am. Chem. Soc.* **2023**, *145*, 15360–15369.

(4) (a) Xu, G.; Elkin, M.; Tantillo, D. J.; Newhouse, T. R.; Maimone, T. J. Traversing Biosynthetic Carbocation Landscapes in the Total Synthesis of Andrastin and Terretonin Meroterpenes. *Angew. Chem., Int. Ed.* **2017**, *56*, 12498–12502. (b) Zhao, Y.; Hu, J.; Chen, R.; Xiong, F.; Xie, H.; Ding, H. Divergent Total Syntheses of (−)-Crinipellins Facilitated by a HAT-Initiated Dowd-Beckwith Rearrangement. *J. Am. Chem. Soc.* **2022**, *144*, 2495–2500.

(5) (a) Discolo, C. A.; Touney, E. E.; Pronin, S. V. Catalytic Asymmetric Radical-Polar Crossover Hydroalkoxylation. *J. Am. Chem. Soc.* **2019**, *141*, 17527–17532. (b) Qin, T.; Lv, G.; Miao, H.; Guan, M.; Xu, C.; Zhang, G.; Xiong, T.; Zhang, Q. Cobalt-Catalyzed Asymmetric Alkylation of (Hetero)Arenes with Styrenes. *Angew. Chem., Int. Ed.* **2022**, *61*, e202201967. (c) Miao, H.; Guan, M.; Xiong, T.; Zhang, G.; Zhang, Q. Cobalt-Catalyzed Enantioselective Hydroamination of Arylalkenes with Secondary Amines. *Angew. Chem., Int. Ed.* **2023**, *62*, e202213913.

(6) (a) Sun, H.-L.; Yang, F.; Ye, W.-T.; Wang, J.-J.; Zhu, R. Dual Cobalt and Photoredox Catalysis Enabled Intermolecular Oxidative Hydrofunctionalization. *ACS Catal.* **2020**, *10*, 4983–4989. (b) Nakagawa, M.; Matsuki, Y.; Nagao, K.; Ohmiya, H. A Triple Photoredox/Cobalt/Brønsted Acid Catalysis Enabling Markovnikov Hydroalkoxylation of Unactivated Alkenes. *J. Am. Chem. Soc.* **2022**, *144*, 7953–7959.

(7) The related two-component cobalt(salen)-catalyzed process that proceeds through an intramolecular radical cyclization is rare: (a) Bamhaoud, T.; Prandi, J. Cobalt-Catalysed Radical Oxygenation with Molecular Oxygen. *Chem. Commun.* **1996**, 1229–1230. (b) Désiré, J.; Prandi, J. A New Synthesis of Carbapentofuranoses from Carbohydrates. *Tetrahedron Lett.* **1997**, *38*, 6189–6192.

(8) The alkylcobatl(IV) intermediate could also be accessed by the alkyl radical addition to Co(II) with subsequent single electron oxidation of the intermediate alkylcobalt(III).

(9) (a) Vitaku, E.; Smith, D. T.; Njardarson, J. T. Analysis of the Structural Diversity, Substitution Patterns, and Frequency of Nitrogen Heterocycles among U.S. FDA Approved Pharmaceuticals. *J. Med. Chem.* **2014**, *57*, 10257–10274. (b) Brown, D. G.; Bostrom, J. Where Do Recent Small Molecule Clinical Development Candidates Come From? *J. Med. Chem.* **2018**, *61*, 9442–9468.

(10) (a) Mao, R.; Frey, A.; Balon, J.; Hu, X. Decarboxylative C(sp^3)–N cross-coupling via synergetic photoredox and copper catalysis. *Nat. Catal.* **2018**, 1, 120–126; (b) Lyang, Y.; Zhang, X.; MacMillan, D. W. C. Decarboxylative sp^3 C–N coupling via dual copper and photoredox catalysis. *Nature* **2018**, *559*, 83–88. (c) Nguyen, V. T.; Nguyen, V. D.; Haug, G. C.; Vuong, N. T. H.; Dang, H. T.; Arman, H. D.; Larionov, O. V. Visible-Light-Enabled Direct Decarboxylative N-Alkylation. *Angew. Chem., Int. Ed.* **2020**, *59*, 7921–7927. (d) Kong, D.; Moon, P. J.; Bsharat, O.; Lundgren, R. J. Direct Catalytic Decarboxylative Amination of Aryl Acetic Acids. *Angew. Chem., Int. Ed.* **2020**, *59*, 1313–1319. (d) Zheng, Y.; Huang, W.; Dhungana, R. K.; Granados, A.; Keess, S.; Makvandi, M.; Molander, G. A. Photochemical Intermolecular [3σ + 2σ]-Cycloaddition for the Construction of Aminobicyclo[3.1.1]heptanes. *J. Am. Chem. Soc.* **2022**, *144*, 23685–23690.

(11) (a) Ricci, A. *Amino Group Chemistry: From Synthesis to the Life Sciences*; John Wiley & Sons, 2008. (b) Roughley, S. D.; Jordan, A. M. The Medicinal Chemist's Toolbox: An Analysis of Reactions Used in the Pursuit of Drug Candidates. *J. Med. Chem.* **2011**, *54*, 3451–3479.

(12) (a) Takeuchi, R.; Ue, N.; Tanabe, K.; Yamashita, K.; Shiga, N. Iridium Complex-Catalyzed Allylic Amination of Allylic Esters. *J. Am. Chem. Soc.* **2001**, *123*, 9525–9534. (b) Ozawa, F.; Okamoto, H.; Kawagishi, S.; Yamamoto, S.; Minami, T.; Yoshifuji, M. (π-Allyl)palladium Complexes Bearing Diphosphinidenecyclobutene Ligands (DPCB): Highly Active Catalysts for Direct Conversion of Allylic Alcohols. *J. Am. Chem. Soc.* **2002**, *124*, 10968–10969. (c) Arnold, J. S.; Nguyen, H. M. Rhodium-Catalyzed Dynamic Kinetic Asymmetric Transformations of Racemic Tertiary Allylic Trichloroacetimidates with Anilines. *J. Am. Chem. Soc.* **2012**, *134*, 8380–8383. (d) Lee, N. R.; Moghadam, F. A.; Braga, F. C.; Lippincott, D. J.; Zhu, B.; Gallou, F.; Lipshutz, B. H. Sustainable Palladium-Catalyzed Tsuji-Trost Reactions Enabled by Aqueous Micellar Catalysis. *Org. Lett.* **2020**, *22*, 4949–4954.

(13) For other approaches to allylic amines, see: (a) Overman, L. E.; Carpenter, N. E. The Allylic Trihaloacetimidate Rearrangement. *Org. React.* **2005**, *66*, 1–107. (b) Bao, H.; Tambar, U. K. Catalytic Enantioselective Allylic Amination of Unactivated Terminal Olefins via an Ene Reaction/[2,3]-Rearrangement. *J. Am. Chem. Soc.* **2012**, *134*, 18495–18498. (c) Sharma, A.; Hartwig, J. F. Enantioselective Functionalization of Allylic C–H Bonds Following a Strategy of Functionalization and Diversification. *J. Am. Chem. Soc.* **2013**, *135*, 17983–17989. (d) Bao, H.; Bayeh, L.; Tambar, U. K. Regioselective and diastereoselective aminoarylation of 1,3-dienes. *Chem. Sci.* **2014**, *5*, 4863–4867. (e) Zhang, Z.; Du, H.; Xu, J.; Li, P. Anti-Markovnikov Rearrangement in Sulfur Mediated Allylic C–H Amination of Olefins. *Chem. Commun.* **2016**, *52*, 11547–11550. (f) Burman, J. S.; Blakey, S. B. Regioselective Intermolecular Allylic C–H Amination of Disubstituted Olefins via Rhodium/π–Allyl Intermediates. *Angew. Chem., Int. Ed.* **2017**, *56*, 13666–13669. (g) Alderson, J. M.; Corbin, J. R.; Schomaker, J. M. Tunable, Chemo- and Site-Selective Nitrene Transfer Reactions through the Rational Design of Silver(I) Catalysts. *Acc. Chem. Res.* **2017**, *50*, 2147–2158. (h) Kohler, D. G.; Gockel, S. N.; Kennemur, J. L.; Waller, P. J.; Hull, K. L. Palladium-Catalysed anti-Markovnikov Selective Oxidative Amination. *Nat. Chem.* **2018**, *10*, 333–40. (i) Bhakta, U.; Kattamuri, P. V.; Siitonen, J. H.; Alemany, L. B.; Kürti, L. Enantioselective Catalytic Allylation of Acyclic Ketiminoesters: Synthesis of α-Fully-Substituted Amino Esters. *Org. Lett.* **2019**, *21*, 9208–9211. (j) Cheng, Q.; Chen, J.; Lin, S.; Ritter, T. Allylic Amination of Alkenes with Iminothianthrenes to Afford Alkyl Allylamines. *J. Am. Chem. Soc.* **2020**, *142*, 17287–17293. (k) Lei, H.; Rovis, T. *Nat. Chem.* **2020**, *12*, 725–731. (l) Ali, S. Z.; Budaitis, B. G.; Fontaine, D. F. A.; Pace, A. L.; Garwin, J. A.; White, M. C. Allylic C–H amination cross-coupling furnishes tertiary amines by electrophilic metal catalysis. *Science* **2022**, *376*, 276–283. (m) Pak Shing Cheung, K.; Fang, J.; Mukherjee, K.; Mihranyan, A.; Gevorgyan, V. Asymmetric intermolecular allylic C–H amination of alkenes with aliphatic amines. *Science* **2022**, *378*, 1207–1213.

(14) (a) Maryanoff, B. E.; Reitz, A. B. The Wittig olefination reaction and modifications involving phosphoryl-stabilized carbanions. Stereochemistry, mechanism, and selected synthetic aspects. *Chem. Rev.* **1989**, *89*, 863–927. (b) Bilel, H.; Hamdi, N.; Zagrouba, F.; Fischmeister, C.; Bruneau, C. Terminal conjugated dienes via a ruthenium-catalyzed cross-metathesis/elimination sequence: Application to renewable resources. *Catal. Sci. Technol.* **2014**, *4*, 2064–2071. (c) Nguyen, V. T.; Dang, H. T.; Pham, H. H.; Nguyen, V. D.; Flores-Hansen, C.; Arman, H. D.; Larionov, O. V. Highly Regio- and Stereoselective Catalytic Synthesis of Conjugated Dienes and Polyenes. *J. Am. Chem. Soc.* **2018**, *140*, 8434–8438. (d) Soengas, R. G.; Rodríguez-Solla, H. Modern Synthetic Methods for the Stereoselective Construction of 1,3-Dienes. *Molecules* **2021**, *26*, 249.

(15) Griesbaum, K.; Behr, A.; Biedenkapp, D.; Voges, H.-W.; Garbe, D.; Paetz, C.; Collin, G.; Mayer, D.; Höke, H.; Schmidt, R. Hydrocarbons. In *Ullmann's Encyclopedia of Industrial Chemistry*, Wiley, 2013, pp 1–61.

(16) (a) Patel, B. A.; Dickerson, J. E.; Heck, R. F. Palladium-Catalyzed Arylation of Conjugated Dienes. *J. Org. Chem.* **1978**, *43*, 5018–5020. (b) Stakem, F. G.; Heck, R. F. Reactions of π-Allylic Palladium Intermediates with Amines. *J. Org. Chem.* **1980**, *45*, 3584–3593. (c) O'Connor, J. M.; Stallman, B. J.; Clark, W. G.; Shu, A. Y. L.; Spada, R. E.; Stevenson, T. M.; Dieck, H. A. Some Aspects of Palladium-Catalyzed Reactions of Aryl and Vinylic Halides with Conjugated Dienes in the Presence of Mild Nucleophiles. *J. Org. Chem.* **1983**, *48*, 807–809. (d) Larock, R. C.; Berrios-Pena, N.; Narayanan, K. Palladium-Catalyzed Heteroannulation of 1,3-Dienes by Functionally Substituted Aryl Halides. *J. Org. Chem.* **1990**, *55*, 3447–3450. (e) Bai, L.; Wang, Y.; Ge, Y.; Liu, J.; Luan, X. Diastereoselective Synthesis of Dibenzo[*b*,*d*]azepines by Pd(II)-Catalyzed [5 + 2] Annulation of *o*-Arylanilines with Dienes. *Org. Lett.* **2017**, *19*, 1734–1737.

(17) (a) Huang, H.-M.; Koy, M.; Serrano, E.; Pflüger, P. M.; Schwarz, J. L.; Glorius, F. Catalytic Radical Generation of π-Allylpalladium Complexes. *Nat. Catal.* **2020**, *3*, 393–400. (b) Huang, H.-M.; Bellotti, P.; Pflueger, P. M.; Schwarz, J. L.; Heidrich, B.; Glorius, F. A Three-Component, Interrupted Radical Heck/Allylic Substitution Cascade Involving Unactivated Alkyl Bromides. *J. Am. Chem. Soc.* **2020**, *142*, 10173–10183. See also: (c) Zheng, Y.; Lu, W.; Xie, Z.; Chen, K.; Xiang, H.; Yang, H. Visible-Light-Induced, Palladium-Catalyzed Annulation of 1,3-Dienes to Construct Vinyl *N*-Heterocycles. *Org. Lett.* **2022**, *24*, 5407–5411.

(18) (a) Okumura, M.; Shved, A. S.; Sarlah, D. Palladium-Catalyzed Dearomative *syn*-1,4-Carboamination. *J. Am. Chem. Soc.* **2017**, *139*, 17787–17790. (b) Chen, S.-S.; Wu, M.-S.; Han, Z.-Y. Palladium-Catalyzed Cascade sp^2 C–H Functionalization/Intramolecular Asymmetric Allylation: From Aryl Ureas and 1,3-Dienes to Chiral Indolines. *Angew. Chem., Int. Ed.* **2017**, *56*, 6641–6645. (c) Pinkert, T.; Wegner, T.; Mondal, S.; Glorius, F. Intermolecular 1,4-Carboamination of Conjugated Dienes Enabled by Cp^*Rh^{III}-Catalyzed C–H Activation. *Angew. Chem., Int. Ed.* **2019**, *58*, 15041–15045. (d) Gosset C.; Moncomble, A.; Dumont C.; Pellegrini, S.; Bousquet, T.; Sauthier, M.; Pélinski, L. Photocatalyzed Amidoarylation of 1,3-Butadiene. *Adv. Synth. Catal.* **2020**, *362*, 3100–3104.

(19) For a review, see: Wu, X.; Gong, L.-Z. Palladium(0)-Catalyzed Difunctionalization of 1,3-Dienes: From Racemic to Enantioselective. *Synthesis* **2019**, *51*, 122–134.

(20) Böttcher, T. J. An Additive Definition of Molecular Complexity. *Chem. Inf. Model.* **2016**, *56*, 462–470.

(21) Wei, W.; Cherukupalli, S.; Jing, L.; Liu, X.; Zhan, P. Fsp^3: A new parameter for drug-likeness. *Drug Discovery Today* **2020**, *25*, 1839–1845.

(22) Sauer, W. H. B.; Schwarz, M. K. Molecular shape diversity of combinatorial libraries: a prerequisite for broad diversity. *J. Chem. Inf. Model.* **2003**, *43*, 987–1003.

(23) (a) Nguyen, V. D.; Haug, G. C.; Greco, S. G.; Trevino, R.; Karki, G. B.; Arman, H. D.; Larionov, O. V. Decarboxylative Sulfinylation Enables a Direct, Metal-Free Access to Sulfoxides from Carboxylic Acids. *Angew. Chem., Int. Ed.* **2022**, e202210525. (b) Dang, H. T.; Nguyen, V. D.; Haug, G. C.; Arman, H. D.; Larionov, O. V. Decarboxylative Triazolation Enables Direct Construction of Triazoles from Carboxylic Acids. *JACS Au* **2023**, *3*, 813–822.

(24) For recent direct decarboxylative functionalizations, see: (a) Kautzky, J. A.; Wang, T.; Evans, R. W.; MacMillan, D. W. C. Decarboxylative Trifluoromethylation of Aliphatic Carboxylic Acids. *J. Am. Chem. Soc.* **2018**, *140*, 6522–6526. (b) Till, N. A.; Smith, R. T.; MacMillan, D. W. C. Decarboxylative Hydroalkylation of Alkynes. *J. Am. Chem. Soc.* **2018**, *140*, 5701–5705. (c) Sun, X.; Chen, J.; Ritter, T. Catalytic Dehydrogenative Decarboxyolefination of Carboxylic Acids. *Nat. Chem.* **2018**, *10*, 1229–1233. (d) Cartwright, K. C.; Lang, S. B.; Tunge, J. A. Photoinduced Kochi Decarboxylative Elimination for the Synthesis of Enamides and Enecarbamates from *N*-Acyl Amino Acids. *J. Org. Chem.* **2019**, *84*, 2933–2940. (e) Faraggi, T. M.; Li, W.; MacMillan, D. W. C. Decarboxylative Oxygenation *via* Photoredox Catalysis. *Isr. J. Chem.* **2020**, *60*, 410–415. (f) Li, J.; Huang, C. Y.; Han, J. T.; Li, C.-J. Development of a Quinolinium/Cobaloxime Dual Photocatalytic System for Oxidative C–C Cross-Couplings *via* H_2 Release. *ACS Catal.* **2021**, *11*, 14148–14158. (g) Kong, D.; Munch, M.; Qiqige, Q.; Cooze, C. J. C.; Rotstein, B. H.; Lundgren, R. J. Fast Carbon Isotope Exchange of Carboxylic Acids Enables by Organic Photoredox Catalysis. *J. Am. Chem. Soc.* **2021**, *143*, 2200–2206. (h) Li, Q. Y.; Gockel, S. N.; Lutovsky, G. A.; DeGlopper, K. S.; Baldwin, N. J.; Bundesmann, M. W.; Tucker, J. W.; Bagley, S. W.; Yoon, T. P. Decarboxylative Cross-Nucleophile Coupling *via* Ligand-to-Metal Charge Transfer Photoexcitation of Cu(II) Carboxylates. *Nat. Chem.* **2022**, *14*, 94–99. (i) Kitcatt, D. M.; Nicolle, S.; Lee, A.-L. Direct Decarboxylative Giese Reactions. *Chem. Soc. Rev.* **2022**, *51*, 1415–1453. For other examples, see: (j) Shang, R.; Liu, L. Transition Metal-Catalyzed Decarboxylative Cross-Coupling Reactions. *Sci. China Chem.* **2011**, *54*, 1670–1687. (k) Wang, J.; Qin, T.; Chen, T.-E.; Wimmer, L.; Edwards, J. T.; Cornella, J.; Vokits, B.; Shaw, S. A.; Baran, P. S. Nickel-Catalyzed Cross-Coupling of Redox-Active Esters with Boronic Acids. *Angew. Chem., Int. Ed.* **2016**, *55*, 9676–9679. (l) Candish, L.; Teders, M.; Glorius, F. Transition-Metal-Free, Visible-Light-Enabled Decarboxylative Borylation of Aryl *N*-Hydroxyphthalimide Esters. *J. Am. Chem. Soc.* **2017**, *139*, 7440–7443. (m) Liu, C.; Shen, N.; Shang. R. Photocatalytic Decarboxylative Alkylation of Silyl Enol Ether and Enamide with *N*-(Acyloxy)phthalimide Using Ammonium Iodide. *Org. Chem. Front.* **2021**, *8*, 4166–4170. (n) Sharique, M.; Majhi, J.; Dhungana, R. K.; Kammer, L. M.; Krumb, M.; Lipp, A.; Romero, E.; Molander, G. A. A Practical and Sustainable Two-Component Minisci Alkylation *via* Photo-Induced EDA-Complex Activation. *Chem. Sci.* **2022**, *13*, 5701–5706.

(25) (a) Nguyen, V. T.; Nguyen, V. D.; Haug, G. C.; Dang, H. T.; Jin, S.; Li, Z.; Flores-Hansen, C.; Benavides, B.; Arman, H. D.; Larionov, O. V. Alkene Synthesis by Photocatalytic Chemoenzymatically Compatible Dehydrodecarboxylation of Carboxylic Acids and Biomass. *ACS Catal.* **2019**, *9*, 9485–9498. (b) Dang, H. T.; Haug, G. C.; Nguyen, V. T.; Vuong, N. T. H.; Arman, H. D.; Larionov, O. V. Acridine Photocatalysis: Insights into the Mechanism and Development of a Dual-Catalytic Direct Decarboxylative Conjugate Addition. *ACS Catal.* **2020**, *10*, 11448–11457. (c) Nguyen, V. T.; Haug, G. C.; Nguyen, V. D.; Vuong, N. T. H.; Arman, H. D.; Larionov, O. V. Photocatalytic Decarboxylative Amidosulfonation Enables Direct Transformation of Carboxylic Acids to Sulfonamides. *Chem. Sci.* **2021**, *12*, 6429–6436. (d) Nguyen, V. T.; Haug, G. C.; Nguyen, V. D.; Vuong, N. T. H.; Karki, G. B.; Arman, H. D.; Larionov, O. V. Functional Group Divergence and The Structural Basis of Acridine Photocatalysis Revealed by Direct Decarboxysulfonylation. *Chem. Sci.* **2022**, *13*, 4170–4179. (e) Nguyen, V. D.; Trevino, R.; Greco, S. G.; Arman, H. D.; Larionov, O. V. Tricomponent Decarboxysulfonylative Cross-coupling Facilitates Direct Construction of Aryl Sulfones and Reveals a Mechanistic Dualism in the Acridine/Copper Photocatalytic System. *ACS Catal.* **2022**, *12*, 8729–8739.

(26) (a) Zubkov, M. O.; Kosobokov, M. D.; Levin, V. V.; Kokorekin, V. A.; Korlyukov, A. A.; Hu, J.; Dilman, A. D. A Novel Photoredox-Active Group for the Generation of Fluorinated Radicals from Difluorostyrenes. *Chem. Sci.* **2020**, *11*, 737–741. (b) Dmitriev, I. A.; Levin, V. V.; Dilman, A. D. Boron Chelates Derived from *N*-Acylhydrazones as Radical Acceptors: Photocatalyzed Coupling of Hydrazones with Carboxylic Acids. *Org. Lett.* **2021**, *23*, 8973–8977. (c) Zubkov, M. O.; Kosobokov, M. D.; Levin, V. V.; Dilman, A. D. Photocatalyzed Decarboxylative Thiolation of Carboxylic Acids Enabled by Fluorinated Disulfide. *Org. Lett.* **2022**, *24*, 2354–2358. (d) Zhilyaev, K. A.; Lipilin, D. L.; Kosobokov, M. D.; Samigullina, A. I.; Dilman, A. D. Preparation and Evaluation of Sterically Hindered Acridine Photocatalysts. *Adv. Synth. Catal.* **2022**, *364*, 3295–3301. (e) Adili, A.; Korpusik, A. B.; Seidel, D.; Sumerlin, B. S. Photocatalytic Direct Decarboxylation of Carboxylic Acids to Derivatize or Degrade Polymers. *Angew. Chem., Int. Ed.* **2022**, *61*, e202209085. (f) Kim, J.; Sun, X.; van der Worp, B. A.; Ritter, T. Anti-Markovnikov Hydrochlorination and Hydronitrooxylation of α-Olefins Via Visible-Light Photocatalysis. *Nat. Catal.* **2023**, *6*, 196–203.

(27) See Figure S7 in the SI.

(28) Gant, T. G. Using Deuterium in Drug Discovery: Leaving the Label in the Drug. *J. Med. Chem.* **2014**, *57*, 3595–3611. (b) Pirali, T.; Serafini, M.; Cargnin, S.; Genazzani, A. A. Application of Deuterium in Medicinal Chemistry. *J. Med. Chem.* **2019**, *62*, 5276–5297.

(29) Yao, T.; Xiao, H.; Wang, H.; Xu, X. Recent Advances in PROTACs for Drug Targeted Protein Research. *Int. J. Mol. Sci.* **2022**, *23*, 10328.

(30) Michelas, M.; Fliedel, C.; Poli, R. Reversible Homolysis of Metal-Carbon Bonds. In *Comprehensive Organometallic Chemistry IV*, Elsevier Ltd.: Amsterdam, 2021; pp 31–85.

(31) (a) Branchaud, B. P.; Yu, G. X. An example of the persistent radical effect in cobaloxime-mediated radical alkyl-alkenyl cross coupling. *Organometallics* **1993**, *12*, 4262–4264. (b) Demarteau, J.; Debuigne, A.; Detrembleur, C. Organocobalt Complexes as Sources of Carbon-Centered Radicals for Organic and Polymer Chemistries. *Chem. Rev.* **2019**, *119*, 6906–6955.

(32) Given the higher hydrogen bond donating ability of benzoic acid, it can serve as a more efficient inhibitor, due to stronger interactions with the aniline, as observed experimentally. Roenfanz, H. F.; Paniak, T. J.; Berlin, C. B.; Tran, V.; Francisco, K. R.; Lassalas, P.; Devas, A.; Landes, O.; Rosenberger, A.; Rotella, M. E.; Ballatore, C.; Kozlowski, M. C. Hydrogen Bonding Parameters by Rapid Colorimetric Assessment: Evaluation of Structural Components Found in Biological Ligands and Organocatalysts. *Chem. Eur. J.* **2023**, *29*, e202300696.

(33) See Figure S27 in SI.

(34) Bickelhaupt, F. M.; Houk, K. N. Analyzing Reaction Rates with the Distortion/Interaction–Activation Strain Model. *Angew. Chem., Int. Ed*. **2017**, *56*, 10070–10086.

(35) Horn, P. R.; Mao, Y.; Head-Gordon, M. Probing non-covalent interactions with a second-generation energy decomposition analysis using absolutely localized molecular orbitals. *Phys. Chem. Chem. Phys.* **2016**, *18*, 23067.

(36) Ramos-Cordoba, E.; Postils, V.; Salvador, P. Oxidation States from Wave Function Analysis. *J. Chem. Theory Comput.* **2015**, *11*, 1501–1508.

(37) Knizia, G. Intrinsic Atomic Orbitals: An Unbiased Bridge Between Quantum Theory and Chemical Concepts. *J. Chem. Theory Comput.* **2013**, *9*, 4834–4843.

(38) (a) Steen, J. S.; Knizia, G.; Klein, J. E. M. N. σ-Noninnocence: Masked Phenyl-Cation Transfer at Formal Ni^{IV}. *Angew. Chem., Int. Ed.* **2019**, *58*, 13133–13139. (b) DiMucci, I. M.; Lukens, J. T.; Chatterjee, S.; Carsch, K. M.; Titus, C. J.; Lee, S. J.; Nordlund, D.; Betley, T. A.; MacMillan, S. N.; Lancaster, K. M. The Myth of d^8 Copper(III). *J. Am. Chem. Soc.* **2019**, *141*, 18508–18520.